Elastic wavefield imaging using the energy norm

Daniel Rocha[1], Nicolay Tanushev[2] & Paul Sava[1]
[1]*Center for Wave Phenomena, Colorado School of Mines*
[2]*Z-Terra, Inc*

ABSTRACT

From the elastic wave equation and the energy conservation principle, we derive an *energy norm* that is applicable to elastic wavefields. Extending the concept of the norm to an inner product enables us to compare two related wavefields. The inner product of source and receiver wavefields at each spatial location leads to an imaging condition. This new imaging condition outputs a single image representing the total reflection energy, and contains individual terms related to the kinetic and strain energy from both extrapolated wavefields. An advantage of the proposed imaging condition compared to alternatives is that it does not suffer from polarity reversal at normal incidence, as do the conventional images using converted waves. This imaging condition also accounts for the directionality of the wavefields in space and time. Based on this, we modify the imaging condition for attenuation of backscattering artifacts in elastic reverse-time migration images. Numerical experiments show the quality of the energy images compared to their conventional counterparts, and the effectiveness of the imaging condition in attenuating backscattering artifacts.

Key words: imaging condition, conservation of energy, elastic imaging, reverse time migration

1 INTRODUCTION

Seismic wavefield imaging is usually implemented using the acoustic wave-equation, based on the inaccurate assumption that only compressional waves propagate in the subsurface. The search for more authentic images and for subsurface information such as fracture distribution drives the development of wavefield imaging using the elastic wave equation. Multicomponent seismic recording and improved computer resources have made wavefield elastic imaging possible (Yan and Xie, 2012).

For both acoustic and elastic cases, wave-equation migration consists of two steps: wavefield extrapolation in the subsurface, using data recorded at the surface, and the application of an imaging condition with the purpose of extracting the Earth's reflectivity from wavefields (Claerbout, 1971; Dellinger and Etgen, 1990; Yan and Sava, 2009). If a two-way elastic wave equation is used in the wavefield extrapolation step, followed by an imaging condition representing zero-lag crosscorrelation between the wavefields, the imaging procedure is called elastic reverse time migration (RTM) (Hokstad et al., 1998). Exploiting the multicomponent aspect of the elastic wavefield, and the possibility of decomposing the displacement fields into P- and S-wave modes, many elastic imaging conditions have been proposed in recent years (Etgen, 1988; Zhe and Greenhalg, 1997; Yan and Sava, 2007; Yan and Xie, 2010; Duan and Sava, 2014a). Correlating the displacement fields for each component of the source and receiver wavefields leads to images with a mixture of P- and S-wave modes, thus making interpretation challenging. In addition, the nine images generated by this imaging condition represent another difficulty for interpretation in 3-D. Alternatively, if the displacement wavefields are separated into P and S waves using Helmholtz decomposition, one can correlate specific wave modes from source and receiver wavefields (Etgen, 1988; Yan and Sava, 2007). Another issue for both displacement and potential imaging conditions is the polarity reversal, which occurs in elastic images due to changes in the elastic wavefield polarization. Specifically, converted waves change sign due to the different orientation of P- and S-polarization vectors in relation to the interface. For isotropic media, this polarity reversal occurs at normal incidence (Balch and Erdermir, 1994), which enables polarity reversal corrections either after angle-domain imaging (Yan and Sava, 2008) or by exploiting the relationship between incidence directions and reflector orientation (Duan and Sava, 2014a).

Considering the issue of polarity reversal and the fact that several images for different wave modes are difficult to interpret, we seek an imaging condition that outputs an attribute of the Earth's reflectivity into a single image. This single im-

age should facilitate interpretation and provide a concise description of the imaged structures. In addition, we intend to assign a clear physical explanation to the imaging condition. As shown in detail elsewhere (Duan and Sava, 2014a; Yan and Sava, 2007), injecting elastic data into a model, implementing back propagation, leads to artifacts. These artifacts might be present even after stacking, masking weak reflections in the final image (Duan and Sava, 2014b).

We propose a new imaging condition that captures all wave modes into a single image, with no polarity reversal at normal incidence. Our imaging condition is derived from the energy conservation principle of an elastic wavefield.

2 THEORY

We use energy conservation laws analogous to the acoustic case to derive a function that measures the energy of a wavefield. This energy function also enables us to form an imaging condition for two extrapolated elastic wavefields.

2.1 Wavefield extrapolation

For an isotropic medium enclosed by a domain $\Omega \subset \mathbb{R}^3$, we can write a wave-equation for the displacement vector with no external sources:

$$\rho \frac{\partial^2 \mathbf{U}}{\partial t^2} = (\lambda + 2\mu) \nabla (\nabla \cdot \mathbf{U}) - \mu \nabla \times (\nabla \times \mathbf{U}) \ . \quad (1)$$

In the equation above, the density and the Lamé parameters are functions of space: $\rho(\mathbf{x})$, $\lambda(\mathbf{x})$, and $\mu(\mathbf{x})$. We assume these parameters vary slowly in Ω, which allows us to disregard their derivatives. The elastic wavefield is a function of space, time and experiment index e: $\mathbf{U}(e, \mathbf{x}, t)$ for $\mathbf{x} \in \Omega$ and $t \in [0, T]$. Assuming Ω is large enough, we can also assume homogeneous boundary conditions for $\mathbf{U}$ and its derivatives, which means $\mathbf{U}$ and its derivatives vanish on the boundary of Ω ($\partial\Omega$) for all $t \in [0, T]$. This is a reasonable assumption because as Ω becomes large enough and the medium has a finite speed of wave propagation, $\mathbf{U}$ becomes close to zero at $\partial\Omega$.

Equation (1) can also be written as a function of velocities by substituting $v_p^2 = \frac{\lambda+2\mu}{\rho}$ and $v_s^2 = \frac{\mu}{\rho}$:

$$\frac{\partial^2 \mathbf{U}}{\partial t^2} = v_p^2 \nabla (\nabla \cdot \mathbf{U}) - v_s^2 \nabla \times (\nabla \times \mathbf{U}) \ . \quad (2)$$

Using the vector calculus identity

$$\nabla \times (\nabla \times \mathbf{U}) = \nabla(\nabla \cdot \mathbf{U}) - \nabla^2 \mathbf{U} \ , \quad (3)$$

we can rewrite equation (2) as

$$\frac{\partial^2 \mathbf{U}}{\partial t^2} = \left(v_p^2 - v_s^2\right) \nabla (\nabla \cdot \mathbf{U}) + v_s^2 \nabla^2 \mathbf{U} \ . \quad (4)$$

2.2 Elastic wavefield energy

The total energy of an acoustic wavefield is conserved (see derivation in Appendix):

$$\dot{E}(t) = \int_\Omega u_t (u_{tt} - c^2 \nabla^2 u) d\mathbf{x} = 0 \ . \quad (5)$$

In this expression, subscript t indicates time derivation. We develop the energy conservation expression for elastic wavefields analogously, by multiplying the time derivative of the wavefield with the wave equation, followed by integration over the whole domain, and then set the expression equal to zero. If we apply the dot product between the wave equation in (4) and $\mathbf{U}_t$, we obtain

$$\mathbf{U}_t \cdot \mathbf{U}_{tt} = \left(v_p^2 - v_s^2\right) \mathbf{U}_t \cdot \nabla (\nabla \cdot \mathbf{U}) + v_s^2 \mathbf{U}_t \cdot \nabla^2 \mathbf{U} \ . \quad (6)$$

Rearranging the term on the left-hand side by the chain rule leads to

$$\frac{1}{2} \frac{d}{dt} |\mathbf{U}_t|^2 = \left(v_p^2 - v_s^2\right) \mathbf{U}_t \cdot \nabla (\nabla \cdot \mathbf{U}) + v_s^2 \mathbf{U}_t \cdot \nabla^2 \mathbf{U} \ , \quad (7)$$

and integrating over the whole domain, we obtain

$$\begin{aligned} \frac{1}{2} \frac{d}{dt} \int_\Omega |\mathbf{U}_t|^2 \, d\mathbf{x} &= \int_\Omega \left(v_p^2 - v_s^2\right) \mathbf{U}_t \cdot \nabla (\nabla \cdot \mathbf{U}) \, d\mathbf{x} \\ &+ \int_\Omega v_s^2 \mathbf{U}_t \cdot \nabla^2 \mathbf{U} \, d\mathbf{x} \ . \end{aligned} \quad (8)$$

We can develop the two terms on the right-hand side of equation (8) separately. For the first term, using integration by parts, we obtain

$$\begin{aligned} &\int_\Omega \left(v_p^2 - v_s^2\right) \mathbf{U}_t \cdot \nabla (\nabla \cdot \mathbf{U}) \, d\mathbf{x} = \\ &\int_\Omega \left(v_p^2 - v_s^2\right) \nabla \cdot \left[\mathbf{U}_t (\nabla \cdot \mathbf{U})\right] \, d\mathbf{x} \\ &- \int_\Omega \left(v_p^2 - v_s^2\right) (\nabla \cdot \mathbf{U}_t) (\nabla \cdot \mathbf{U}) \, d\mathbf{x} \ . \end{aligned} \quad (9)$$

The first term on the right-hand side of equation (9) can be turned into a surface integral by the Divergence Theorem, thus becoming zero; both the wavefield $\mathbf{U}$ and its derivatives vanish on the boundary $\partial\Omega$, as explained in the previous section:

$$\begin{aligned} &\int_\Omega \left(v_p^2 - v_s^2\right) \nabla \cdot \left[\mathbf{U}_t (\nabla \cdot \mathbf{U})\right] d\mathbf{x} = \\ &\int_{\partial\Omega} \left(v_p^2 - v_s^2\right) \left[\mathbf{U}_t (\nabla \cdot \mathbf{U})\right] \cdot \mathbf{n} \, d\mathbf{x} = 0 \ . \end{aligned} \quad (10)$$

Therefore, equation (9) becomes

$$\begin{aligned} &\int_\Omega \left(v_p^2 - v_s^2\right) \mathbf{U}_t \cdot \nabla (\nabla \cdot \mathbf{U}) \, d\mathbf{x} = \\ &- \int_\Omega \left(v_p^2 - v_s^2\right) (\nabla \cdot \mathbf{U}_t) (\nabla \cdot \mathbf{U}) \, d\mathbf{x} \ . \end{aligned} \quad (11)$$

Assuming that the medium parameters v_p^2 and v_s^2 are slowly varying, using the chain rule, we arrange the term on the right-hand side as follows:

$$\int_\Omega \left(v_p^2 - v_s^2\right) \mathbf{U}_t \cdot \nabla \left(\nabla \cdot \mathbf{U}\right) d\mathbf{x} = -\frac{1}{2}\frac{d}{dt}\int_\Omega \left(v_p^2 - v_s^2\right) |\nabla \cdot \mathbf{U}|^2 \, d\mathbf{x} \, . \quad (12)$$

Similarly, for the second term on the right-hand side of equation (8), we use the component-wise application of the Laplacian operator ∇^2 on the vector field $\mathbf{U}$. Then, the application of the dot product leads to the sum of three terms in the form $b_t \nabla^2 b$. For each component of the wavefield, the Green's first identity (see Appendix) is used:

$$\int_\Omega b_t \nabla^2 b \, d\mathbf{x} + \int_\Omega \nabla b_t \cdot \nabla b \, d\mathbf{x} = \int_{\partial\Omega} b_t \frac{\partial b}{\partial n} \, d\mathbf{x} \, , \quad (13)$$

where $\frac{\partial b}{\partial n}$ is the normal derivative of b on $\partial\Omega$. Once more, as the wavefield and its derivatives vanish on the boundary, the left-hand side term goes to zero, yielding

$$\int_\Omega b_t \nabla^2 b \, d\mathbf{x} = -\int_\Omega \nabla b_t \cdot \nabla b \, d\mathbf{x} \, . \quad (14)$$

The gradient operator on a vector results in a matrix, and the dot product on the right-hand side becomes a Frobenius product (see Appendix), which is simply the sum of the products between their corresponding elements. We can, therefore, rewrite the second term on the left-hand side of (8) as

$$\int_\Omega v_s^2 \mathbf{U}_t \cdot \nabla^2 \mathbf{U} \, d\mathbf{x} = -\int_\Omega (\nabla(v_s^2 \mathbf{U}_t)) : (\nabla \mathbf{U}) \, d\mathbf{x} \, . \quad (15)$$

Using the definition of a Frobenius product ($A : B = Tr[AB^T]$), and assuming once more that v_s^2 is slowly varying, we obtain

$$\begin{aligned} \int_\Omega v_s^2 \mathbf{U}_t \cdot \nabla^2 \mathbf{U} \, d\mathbf{x} &= -\int_\Omega v_s^2 (\nabla \mathbf{U}_t) : (\nabla \mathbf{U}) \, d\mathbf{x} \\ &= -\int_\Omega v_s^2 \mathrm{Tr}[\nabla \mathbf{U}_t (\nabla \mathbf{U})^T] \, d\mathbf{x} \\ &= -\frac{1}{2}\int_\Omega v_s^2 \mathrm{Tr}[\nabla \mathbf{U}_t (\nabla \mathbf{U})^T \\ &+ \nabla \mathbf{U}_t (\nabla \mathbf{U})^T] \, d\mathbf{x} \, , \end{aligned} \quad (16)$$

and using the chain rule, we obtain

$$\begin{aligned} - &\frac{1}{2}\int_\Omega v_s^2 \mathrm{Tr}[\nabla \mathbf{U}_t (\nabla \mathbf{U})^{\mathrm{T}} + \nabla \mathbf{U}_t (\nabla \mathbf{U})^{\mathrm{T}}] \, d\mathbf{x} \\ = &-\frac{1}{2}\frac{d}{dt}\int_\Omega v_s^2 \mathrm{Tr}[(\nabla \mathbf{U})(\nabla \mathbf{U})^{\mathrm{T}}] \, d\mathbf{x} \\ = &-\frac{1}{2}\frac{d}{dt}\int_\Omega v_s^2 \|\nabla \mathbf{U}\|_F^2 \, d\mathbf{x} \, , \end{aligned} \quad (17)$$

where $\| \cdot \|_F^2$ is the Frobenius norm.

Rewriting equation (8) with the new right-hand side terms from (12) and (17) leads to

$$\frac{1}{2}\frac{d}{dt}\int_\Omega \left(|\mathbf{U}_t|^2 + \left(v_p^2 - v_s^2\right) |\nabla \cdot \mathbf{U}|^2 + v_s^2 \|\nabla \mathbf{U}\|_F^2\right) \, d\mathbf{x} = 0 \, , \quad (18)$$

and we obtain an expression in the form $\dot{E}(t) = 0$. The function E measures the total energy of the wavefield within a domain:

$$E(t) = \int_\Omega \left(|\mathbf{U}_t|^2 + \left(v_p^2 - v_s^2\right) |\nabla \cdot \mathbf{U}|^2 + v_s^2 \|\nabla \mathbf{U}\|_F^2\right) \, d\mathbf{x} \, . \quad (19)$$

The evaluation of the wavefield energy at each spatial location and time can be obtained by the point-wise energy function:

$$E_{\mathrm{pt}}(\mathbf{x}, t) \equiv |\mathbf{U}_t|^2 + \left(v_p^2 - v_s^2\right) |\nabla \cdot \mathbf{U}|^2 + v_s^2 \|\nabla \mathbf{U}\|_F^2 \, . \quad (20)$$

Considering two wavefields $\mathbf{U}$ and $\mathbf{V}$, we can define an inner product:

$$\begin{aligned} < \mathbf{U}, \mathbf{V} >_E \equiv \int_0^T \int_\Omega \Big[&\mathbf{U}_t \cdot \mathbf{V}_t \\ + &(v_p^2 - v_s^2)(\nabla \cdot \mathbf{U})(\nabla \cdot \mathbf{V}) \\ + &v_s^2 \left(\nabla \mathbf{U}\right) : \left(\nabla \mathbf{V}\right) \Big] d\mathbf{x} dt \, . \end{aligned} \quad (21)$$

2.3 Physical Interpretation

Rewriting the energy function in equation (20) in terms of the density and Lamé parameters, yields

$$E_{\mathrm{pt}}(\mathbf{x}, t) = \rho |\mathbf{U}_t|^2 + (\lambda + \mu) |\nabla \cdot \mathbf{U}|^2 + \mu \|\nabla \mathbf{U}\|_F^2 \, . \quad (22)$$

This equation enables us to interpret the total mechanical energy function in terms of kinetic and potential energies at every point in space and at all times. The first term, composed of the product of density and particle velocity, represents the wavefield kinetic energy (Holstrom, 1968). Under the assumption that the total energy is conserved, the remaining terms of equation (22) can be interpreted as potential energy:

- The $\nabla \cdot \mathbf{U}$ term captures the volumetric strain of the elastic medium deforming under the influence of a passing wave
- The $\|\nabla \mathbf{U}\|_F$ term captures, among other things, the torsional deformation of the elastic solid

The derived imaging condition, based on the energy function given by equation (22) represents the deformation of the elastic solid under investigation, so it can be interpreted as a description of strain.

2.4 Imaging condition

We propose a new elastic imaging condition based on the point-wise inner product in (21) between source and receiver wavefields, followed by integration over time and experi-

ments:

$$I_E = \sum_{e,t} \Big[\mathbf{U}_t \cdot \mathbf{V}_t + \left(v_p^2 - v_s^2\right) (\nabla \cdot \mathbf{U})(\nabla \cdot \mathbf{V}) + v_s^2 \, (\nabla \mathbf{U}) : (\nabla \mathbf{V}) \Big] \, . \quad (23)$$

Here, $\mathbf{U}\,(e, \mathbf{x}, t)$ and $\mathbf{V}\,(e, \mathbf{x}, t)$ are the source and receiver vector wavefields, respectively, and $I_E\,(\mathbf{x})$ is the scalar image. We can describe this imaging condition as a dot product between the following multidimensional vectors:

$$\Box\mathbf{U} = \left\{ \mathbf{U}_t, \sqrt{v_p^2 - v_s^2}(\nabla \cdot \mathbf{U}), v_s(\nabla \mathbf{U}) \right\}, \quad (24)$$

$$\Box\mathbf{V} = \left\{ \mathbf{V}_t, \sqrt{v_p^2 - v_s^2}(\nabla \cdot \mathbf{V}), v_s(\nabla \mathbf{V}) \right\} \, . \quad (25)$$

Equations (24) and (25) define multidimensional vectors with thirteen components, of which three components are the wavefield time derivatives ($\mathbf{U}_t, \mathbf{V}_t$), one is the scaled divergence of the wavefields ($\nabla \cdot \mathbf{U}, \nabla \cdot \mathbf{V}$), and nine are from the tensor wavefield gradient ($\nabla\mathbf{U}, \nabla\mathbf{V}$).

Therefore, we can rewrite equation (23) as

$$I_E = \sum_{e,t} \Box\mathbf{U} \cdot \Box\mathbf{V} \, . \quad (26)$$

This expression is analogous to the similar imaging condition developed for acoustic wavefields (Rocha et al., 2015), and has similar physical interpretation and application, as discussed in the next section.

2.5 Backscattering attenuation

Vectors $\Box\mathbf{U}$ and $\Box\mathbf{V}$ are related to the polarization and propagation direction of the elastic wavefields $\mathbf{U}$ and $\mathbf{V}$. Decomposing the wavefield $\mathbf{U}$ in plane waves, we obtain

$$\mathbf{U} = \mathbf{u}_0 e^{i\omega(\mathbf{p}\cdot\mathbf{x} - t)} \, , \quad (27)$$

where $\mathbf{u}_0$ is the polarization vector, $\mathbf{p}$ is the slowness vector, and ω is the frequency. We assume that ω is large and that the vectors $\mathbf{u}_0$ and $\mathbf{p}$ are slowly varying in space and time, which makes the spatial and temporal derivatives of $\mathbf{u}_0$ and $\mathbf{p}$ small compared to ω. Substituting the plane wave definition (27) into the solution of the elastic equation in (2), we obtain the Christoffel equation for isotropic media (see Appendix):

$$\mathbf{u}_0 = \left(v_p^2 - v_s^2\right) (\mathbf{u}_0 \cdot \mathbf{p})\, \mathbf{p} + v_s^2 \, (\mathbf{p} \cdot \mathbf{p})\, \mathbf{u}_0 \, . \quad (28)$$

Multiplying the equation in (28) by $\mathbf{u}_0$ leads to

$$|\mathbf{u}_0|^2 = \left(v_p^2 - v_s^2\right) (\mathbf{u}_0 \cdot \mathbf{p})^2 + v_s^2 |\mathbf{p}|^2 |\mathbf{u}_0|^2 \, . \quad (29)$$

The terms in equation (29) are present in the norm of $\Box\mathbf{U}$, defined in equation (24):

$$\mathbf{U}_t = -i\omega \mathbf{u}_0 e^{i\omega(\mathbf{p}\cdot\mathbf{x} - t)} \, , \quad (30)$$

$$\nabla \cdot \mathbf{U} = i\omega \, (\mathbf{u}_0 \cdot \mathbf{p})\, e^{i\omega(\mathbf{p}\cdot\mathbf{x} - t)} \, , \quad (31)$$

$$\nabla\mathbf{U} = -i\omega \, (\mathbf{u}_0 \otimes \mathbf{p})\, e^{i\omega(\mathbf{p}\cdot\mathbf{x} - t)} \, , \quad (32)$$

where $\otimes$ indicates the outer product between two vectors, resulting in a matrix. Therefore, the norm of $\Box\mathbf{U}$ is

$$\|\Box\mathbf{U}\|^2 = \Box\mathbf{U} \cdot \Box\mathbf{U} = \mathbf{U}_t \cdot \mathbf{U}_t + \left(v_p^2 - v_s^2\right) (\nabla \cdot \mathbf{U})(\nabla \cdot \mathbf{U}) + v_s^2 \, (\nabla \mathbf{U}) : (\nabla \mathbf{U}) \quad (33)$$

$$= -\omega^2 \Big[|\mathbf{u}_0|^2 + \left(v_p^2 - v_s^2\right) (\mathbf{u}_0 \cdot \mathbf{p})^2 + v_s^2 |\mathbf{p}|^2 |\mathbf{u}_0|^2 \Big] e^{i\omega(\mathbf{p}\cdot\mathbf{x} - t)} \, . \quad (34)$$

We seek to define an imaging condition that attenuates waves propagating along the same path and with the same polarization, i.e., elastic backscattering. Defining $(\Box\mathbf{V})^\dagger$ as

$$(\Box\mathbf{V})^\dagger = \left\{ -\mathbf{V}_t, \sqrt{v_p^2 - v_s^2}(\nabla \cdot \mathbf{V}), v_s(\nabla \mathbf{V}) \right\} \, , \quad (35)$$

we can compute the dot product between $\Box\mathbf{U}$ and $(\Box\mathbf{V})^\dagger$ as

$$\Box\mathbf{U} \cdot (\Box\mathbf{V})^\dagger = -\mathbf{U}_t \cdot \mathbf{V}_t + \left(v_p^2 - v_s^2\right) (\nabla \cdot \mathbf{U})(\nabla \cdot \mathbf{V}) + v_s^2 \, (\nabla \mathbf{U}) : (\nabla \mathbf{V}) \quad (36)$$

$$= \omega^2 \Big[|\mathbf{u}_0|^2 - \left(v_p^2 - v_s^2\right) (\mathbf{u}_0 \cdot \mathbf{p})^2 - v_s^2 |\mathbf{p}|^2 |\mathbf{u}_0|^2 \Big] e^{i\omega(\mathbf{p}\cdot\mathbf{x} - t)} \, . \quad (37)$$

Using the relation in (29), we obtain

$$\Box\mathbf{U} \cdot (\Box\mathbf{V})^\dagger = 0 \, , \quad (38)$$

i.e., the dot product is zero everywhere except at locations where reflectors exist or different wave modes interact, since the vectors $\mathbf{p}$ and $\mathbf{u}_0$ are different for $\mathbf{U}$ and $\mathbf{V}$ at these locations. Therefore, the dot product in equation (38) nullifies the events that propagate on the same path and have the same polarization. Such events include reflection backscattering, diving, direct and head waves from the same wave modes. Therefore, the imaging condition

$$I_E^\dagger = \sum_{e,t} \Box\mathbf{U} \cdot (\Box\mathbf{V})^\dagger \quad (39)$$

attenuates backscattering artifacts in elastic RTM images.

3 EXAMPLES

Using a simple model with a horizontal reflector at $z = 1.5$ km, we test the proposed imaging condition and compare it with the conventional imaging conditions. A vertical displacement source function is used in the experiments shown in Figures 1-3. Figure 1 shows images correlating the displacement components of source and receiver wavefields. Figure 2 shows images correlating the scalar and vector potentials of the wavefields. Note the polarity reversal at normal incidence in Figures 1(b), 1(c), 2(b), and 2(c). Figure 3 shows the three individual energy terms of the imaging condition, and then the sum of these three terms resulting in the energy imaging condition in Figure 3(c).

We repeat the same experiments from Figures 1-3 adding a reflector in the migration velocity (Figures 4, 5, and 6). This

jump in the migration velocity causes backscattering artifacts in elastic RTM images. These artifacts appear most prominently in the images using displacement components (Figure 4), PP (Figure 5(a)) and SS (Figure 5(d)) images. In the PS (Figure 5(b)) and SP (Figure 5(c)) images, the converted reflections do not correlate with the incident waves, thus freeing these images from backscattering artifacts. The energy imaging condition also shows backscattering artifacts (Figure 6(c)). However, using the modified energy imaging condition in equation (39) attenuates the backscattering artifacts (Figure 7).

Figure 8 shows the Marmousi model used to test our new elastic imaging condition. The migration velocity is a smoothed version of the stratigraphic velocity, which is used to generate synthetic data. Using the energy imaging condition in equation (23), we obtain the image in Figure 8(a), which presents backscattering artifacts. We attenuate these artifacts in Figure 8(b) using the imaging condition from equation (39). The individual elastic images for shots do not show polarity reversal at normal incidence, and therefore, stacking is constructive, leading to a good quality image, as seen in Figure 8(b).

4 CONCLUSIONS

The energy imaging condition offers an alternative to the conventional imaging conditions, whice use potentials or displacement components. This alternative combines all wave modes into a single image and does not suffer from polarity reversal, as is the case for conventional images using converted modes, either with potentials or displacements. The energy imaging condition accounts for wavefield directionality, including the wavefield propagation and polarization directions. We describe this imaging condition as the projection between the multidimensional vectors $\Box\mathbf{U}$ and $\Box\mathbf{V}$ (built using the extrapolated wavefields $\mathbf{U}$ and $\mathbf{V}$), whose terms contain information about wavefield directionality. By exploiting this directionality, we are able to attenuate the backscattering artifacts in the imaging, in a way that is similar to the case with acoustic waves.

5 ACKNOWLEDGMENTS

We would like to thank sponsor companies of the Consortium Project on Seismic Inverse Methods for Complex Structures, whose support made this research possible. We acknowledge Yuting Duan, who provided the elastic modeling code for this research. The reproducible numeric examples in this paper use the Madagascar open-source software package (Fomel et al., 2013) freely available from http://www.ahay.org.

REFERENCES

Balch, A. H., and C. Erdermir, 1994, Sign-change correction for prestack migration of P-S converted wave reflections: Geophysical Prospecting, **42**, 637–663.

Claerbout, J. F., 1971, Toward a unified theory of reflector mapping: Geophysics, **36**, 467–481.

Dellinger, J., and J. Etgen, 1990, Wave-field separation in two-dimensional anisotropic media: Geophysics, **55**, 914–919.

Duan, Y., and P. Sava, 2014a, Converted-waves imaging condition for elastic reverse-time migration: Presented at the SEG 2014 Denver Annual Meeting.

———, 2014b, Elastic reverse-time migration with obs multiples: Presented at the SEG 2014 Denver Annual Meeting.

Etgen, J. T., 1988, Prestacked migration of P- and SV-waves: Presented at the SEG 1988 Annual Meeting.

Evans, L. C., 1997, Partial Differential Equations: American Mathematical Society, **19**.

Fomel, S., P. Sava, I. Vlad, Y. Liu, and V. Bashkardin, 2013, Madagascar: open-source software project for multidimensional data analysis and reproducible computational experiments: Journal of Open Research Software, **1**.

Golub, G. H., and C. F. V. Loan, 1996, Chapter 2 - Matrix Analysis, *in* Matrix computations, 3 ed.: John Hopkins University Press.

Hokstad, K., R. Mittet, and M. Landrø, 1998, Elastic reverse time migration of marine walkaway vertical seismic profiling data: Geophysics, **63**, 1685–1695.

Holstrom, G., 1968, Nonlinear energy transfer in elastic waves: Geophysics, **33**, 734–746.

McOwen, R. C., 2003, Partial Differential Equations: Methods and Applications, 2 ed.: Prentice Hall.

Musgrave, M., 1970, Crystal Acoustics: Holden-Day.

Rocha, D., N. Tanushev, and P. Sava, 2015, Acoustic wavefield imaging using the energy norm: Presented at the SEG New Orleans 2015 Annual Meeting.

Tsvankin, I., 2012, Seismic signatures and analysis of reflection data in anisotropic media, 3 ed.: Society of Exploration Geophysicists.

Yan, J., and P. Sava, 2007, Elastic wavefield imaging with scalar and vector potentials: Presented at the SEG Denver 2007 Annual Meeting.

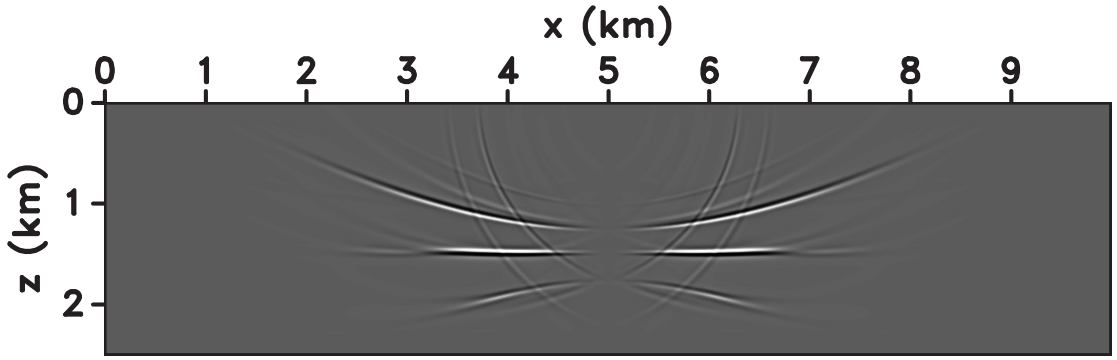
———, 2008, Isotropic angle-domain elastic reverse-time migration: Geophysics, **73**, S229–S239.

———, 2009, Elastic wave-mode separation for VTI media: Geophysics, **74**, WB19–WB32.

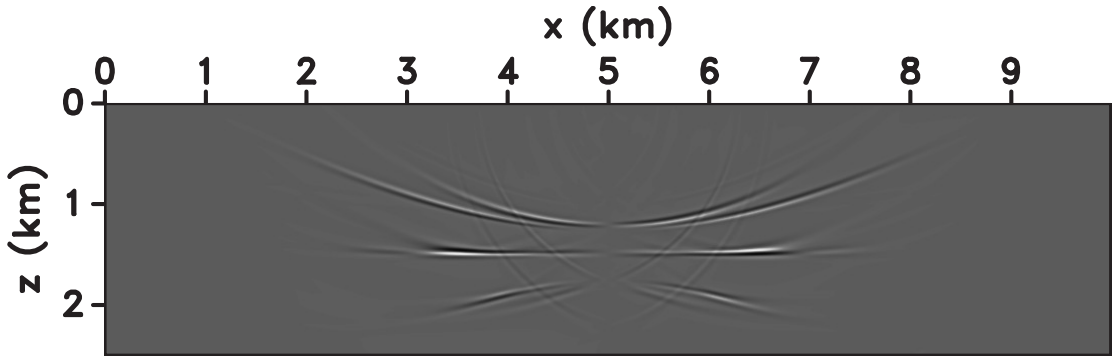
Yan, R., and X.-B. Xie, 2010, The new angle-domain imaging condition for elastic RTM: Presented at the SEG Denver 2010 Annual Meeting.

———, 2012, An angle-domain imaging condition for elastic reverse time migration and its application to angle gather extraction: Geophysics, **77**, S105–S115.

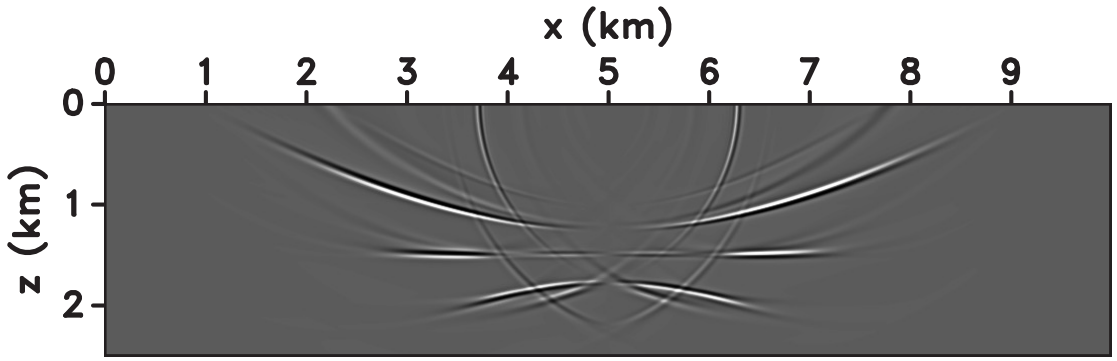
Zhe, J., and S. A. Greenhalg, 1997, Prestack multicomponent migration: Geophysics, **62**, 598–613.



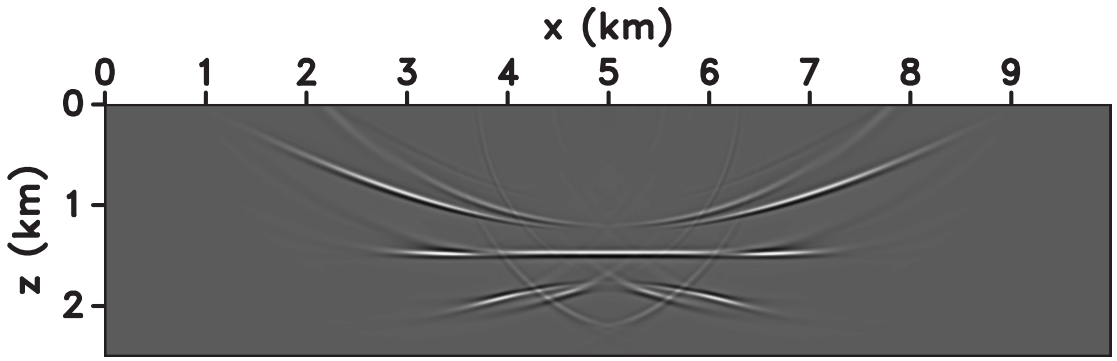
(a)



(b)

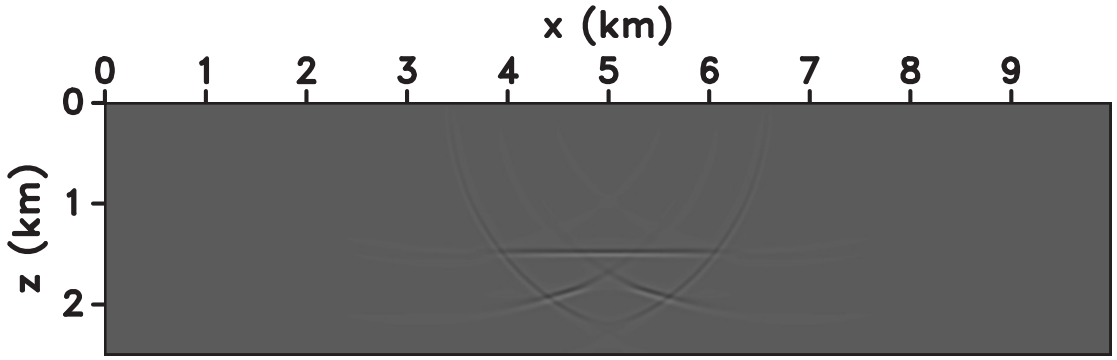


(c)

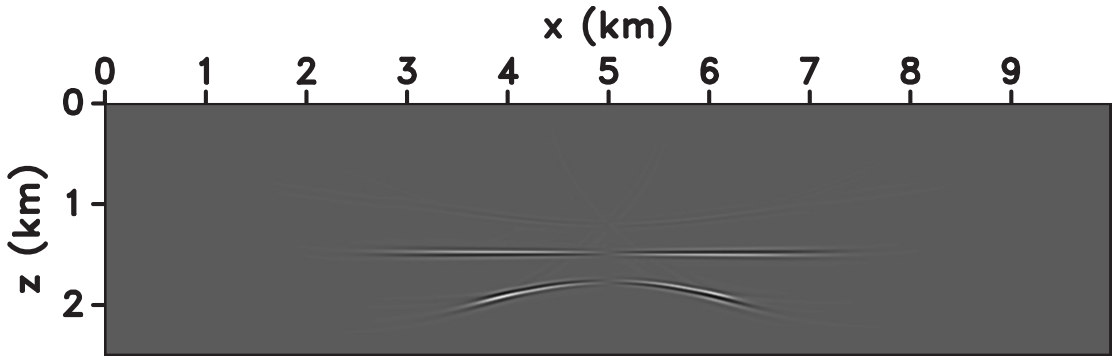


(d)

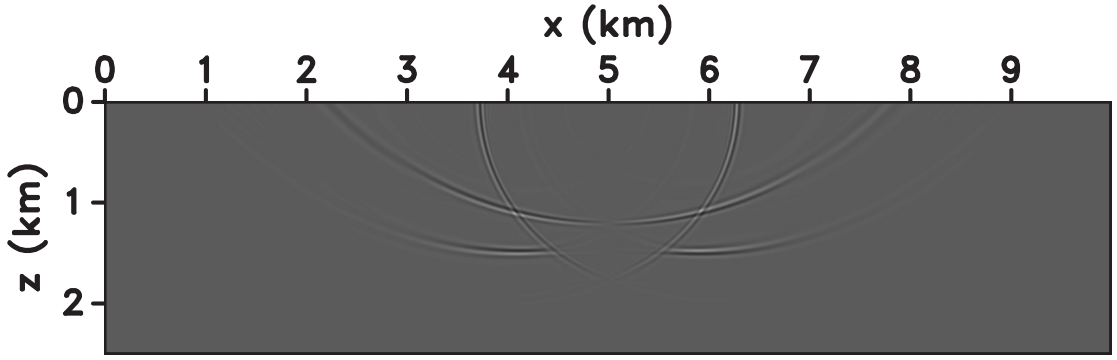
Figure 1. Imaging conditions using displacement components for a horizontal reflector with a vertical displacement source at $x = 5$ km: (a) U_xV_x, (b) U_xV_z, (c) U_zV_x, and (d) U_zV_z image, where $\{U_x, U_z\}$ and $\{V_x, V_z\}$ are the horizontal and vertical components of the source and receiver wavefields, respectively.



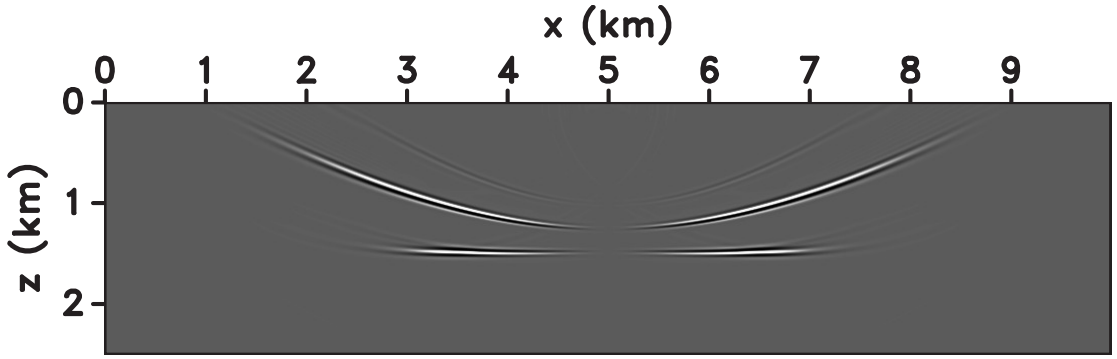
(a)



(b)



(c)



(d)

Figure 2. Imaging conditions using potentials for a horizontal reflector with a vertical displacement source at $x = 5$ km: (a) PP, (b) PS, (c) SP, and (d) SS image. The artifacts in these images occur due to the fake modes, which are generated when injecting the displacement in the receiver wavefield.

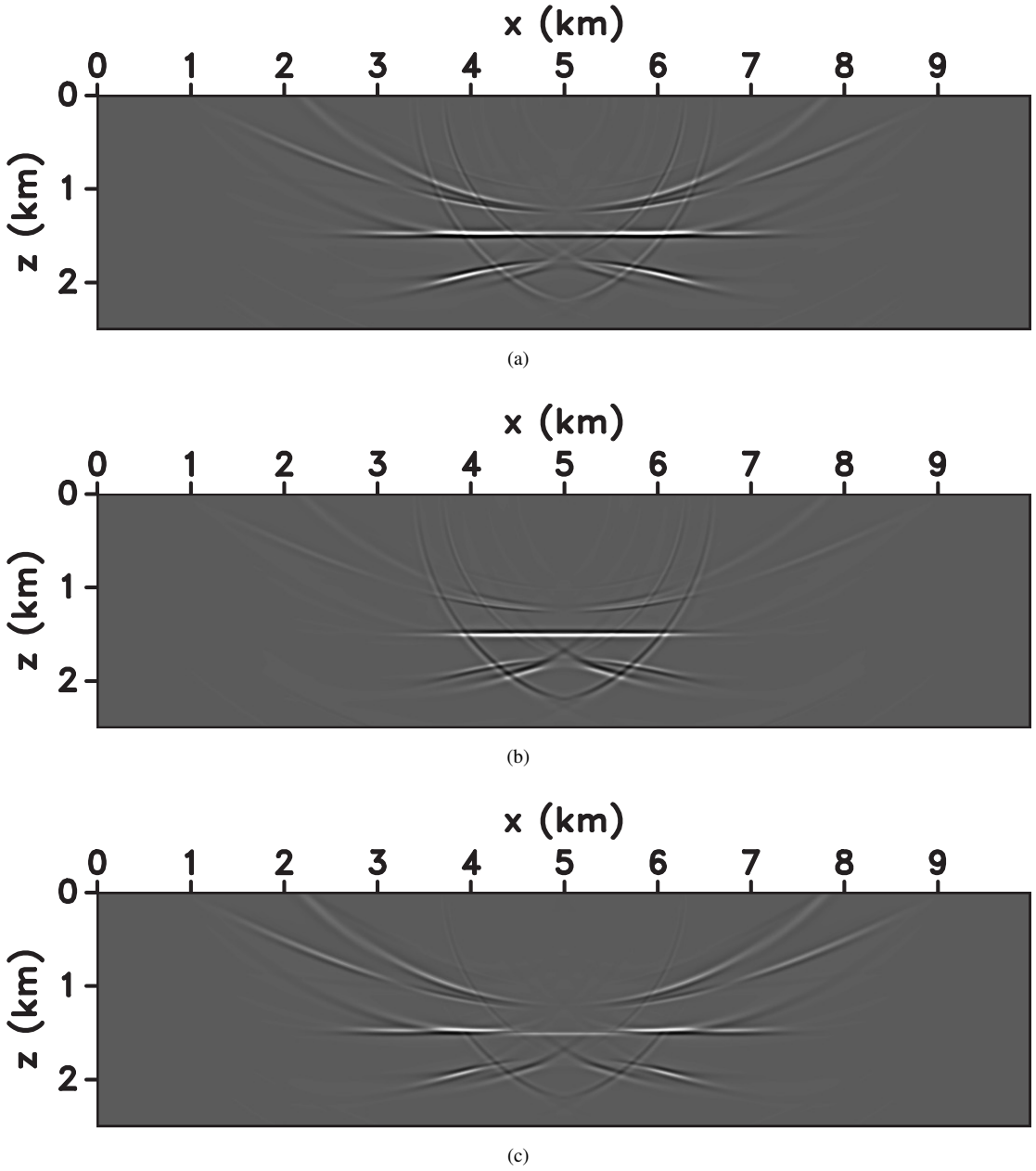


Figure 3. Individual terms of the energy imaging condition for a horizontal reflector with a vertical displacement source: (a) kinetic energy, (b) potential energy, and (c) total energy.

6 APPENDIX

6.1 Divergence Theorem and Green's First Identity

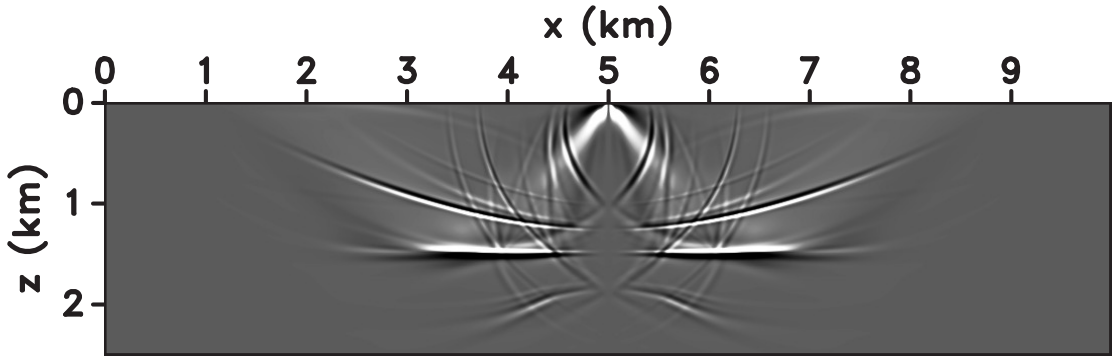
Consider a vector field $\mathbf{F}$. The Divergence Theorem states that

$$\int_{\Omega} (\nabla \cdot \mathbf{F}) d\mathbf{x} = \int_{\partial\Omega} \mathbf{F} \cdot \mathbf{n} \, d\mathbf{x} \, , \tag{A-1}$$

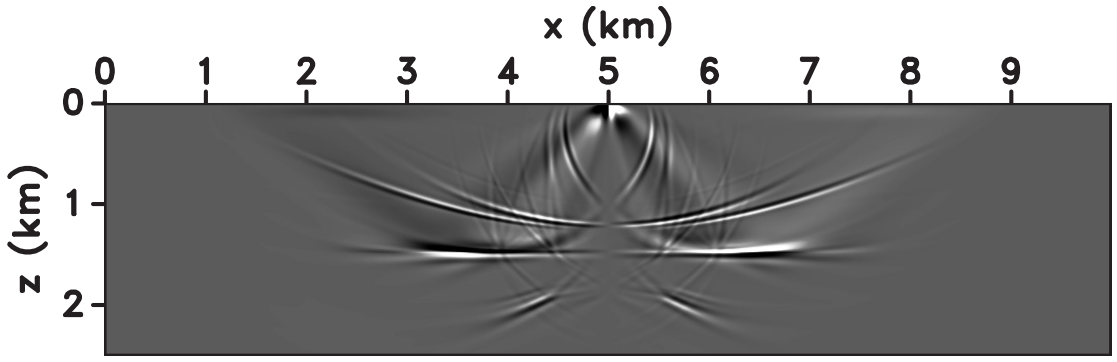
where $\mathbf{n}$ is the outward pointing normal.

For scalar functions $u(\mathbf{x})$ and $v(\mathbf{x})$, we can define the vector field $\mathbf{F} = u\nabla v$. Applying the divergence operator on $\mathbf{F}$:

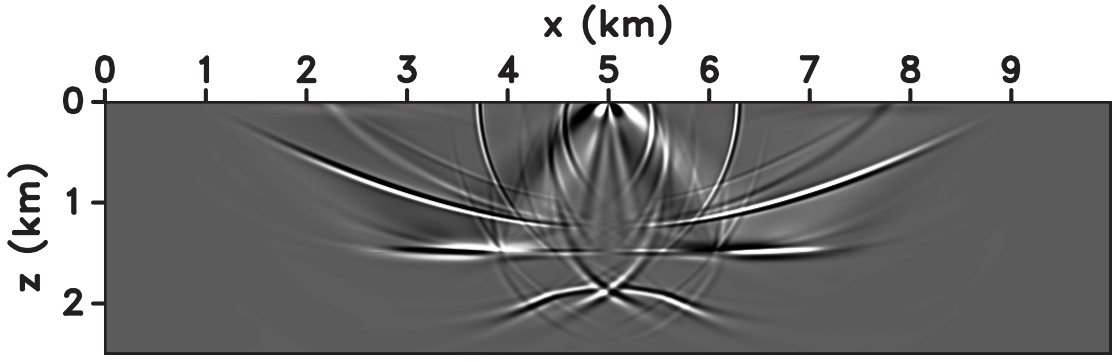
$$\int_{\Omega} u\nabla^2 v d\mathbf{x} + \int_{\Omega} \nabla u \cdot \nabla v d\mathbf{x} = \int_{\Omega} \nabla \cdot (u\nabla v) d\mathbf{x} = \int_{\Omega} \nabla \cdot \mathbf{F} d\mathbf{x} \, , \tag{A-2}$$



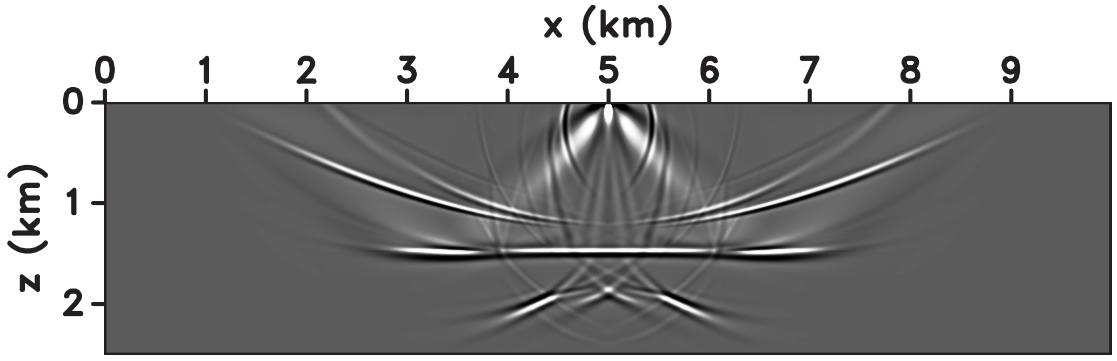
(a)



(b)

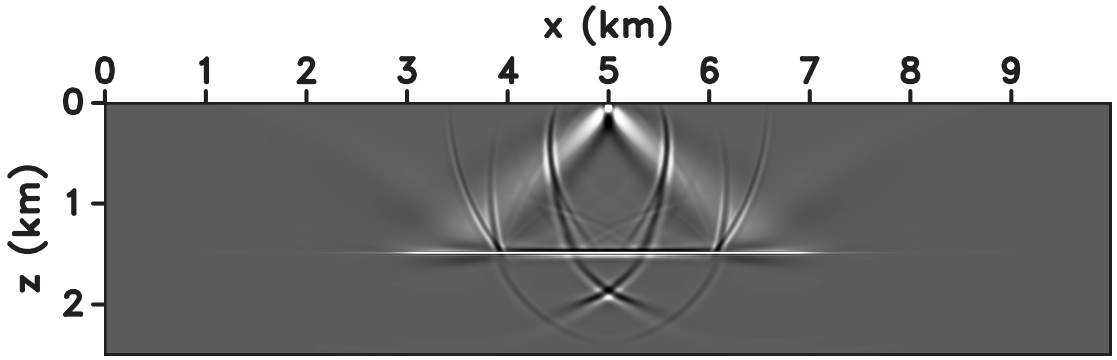


(c)

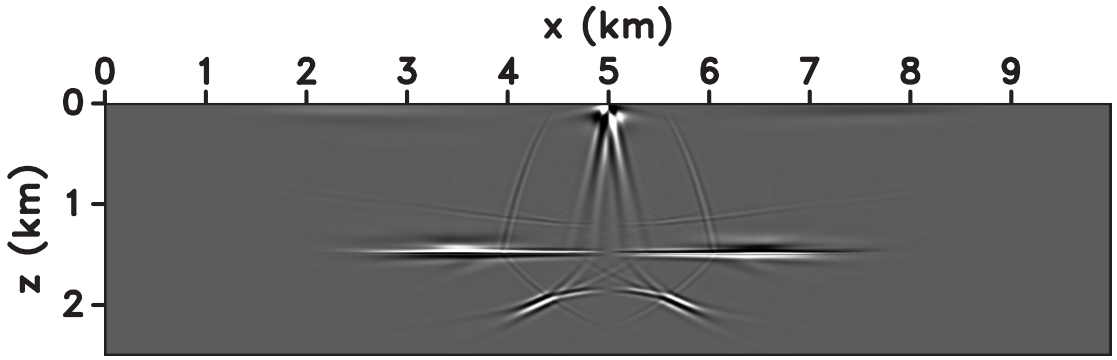


(d)

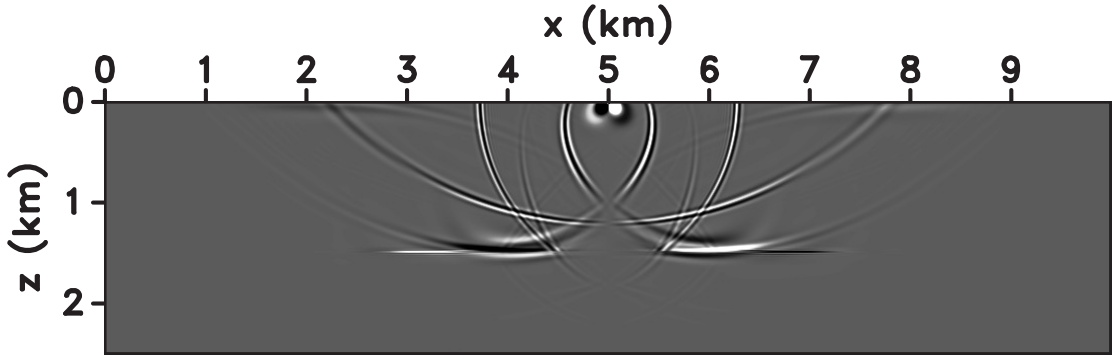
Figure 4. Same experiment of Figure 1 with the reflector present in the migration velocity to generate backscattering artifacts. Images with displacement components: **U** is the source wavefield and **V** is the receiver wavefield: ((a) U_xV_x, (b) U_xV_z, (c) U_zV_x and (d) U_zV_z image, where $\{U_x, U_z\}$ and $\{V_x, V_z\}$ are the horizontal and vertical components of the source and receiver wavefields, respectively.



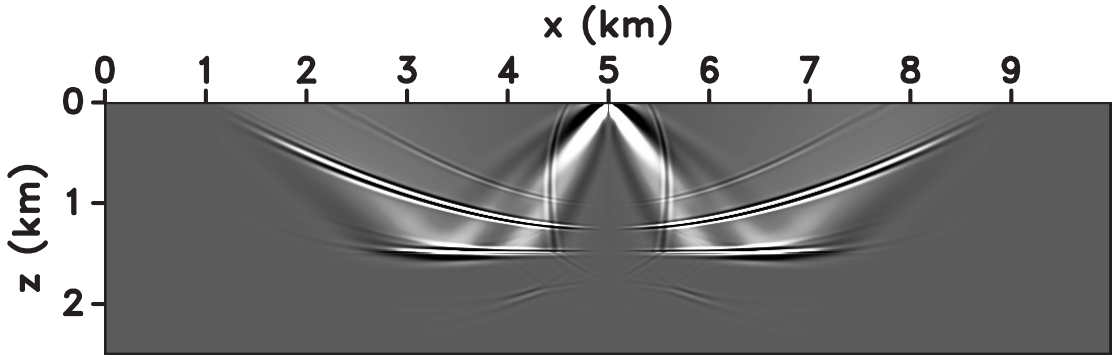
(a)



(b)



(c)



(d)

Figure 5. Same experiment of Figure 2 with the reflector present in the migration velocity to generate backscattering artifacts. Images with scalar and vector potentials: (a) PP, (b) PS, (c) SP and (d) SS image. The correlation between same wave modes in (a) and (d) generate backscattering artifacts.

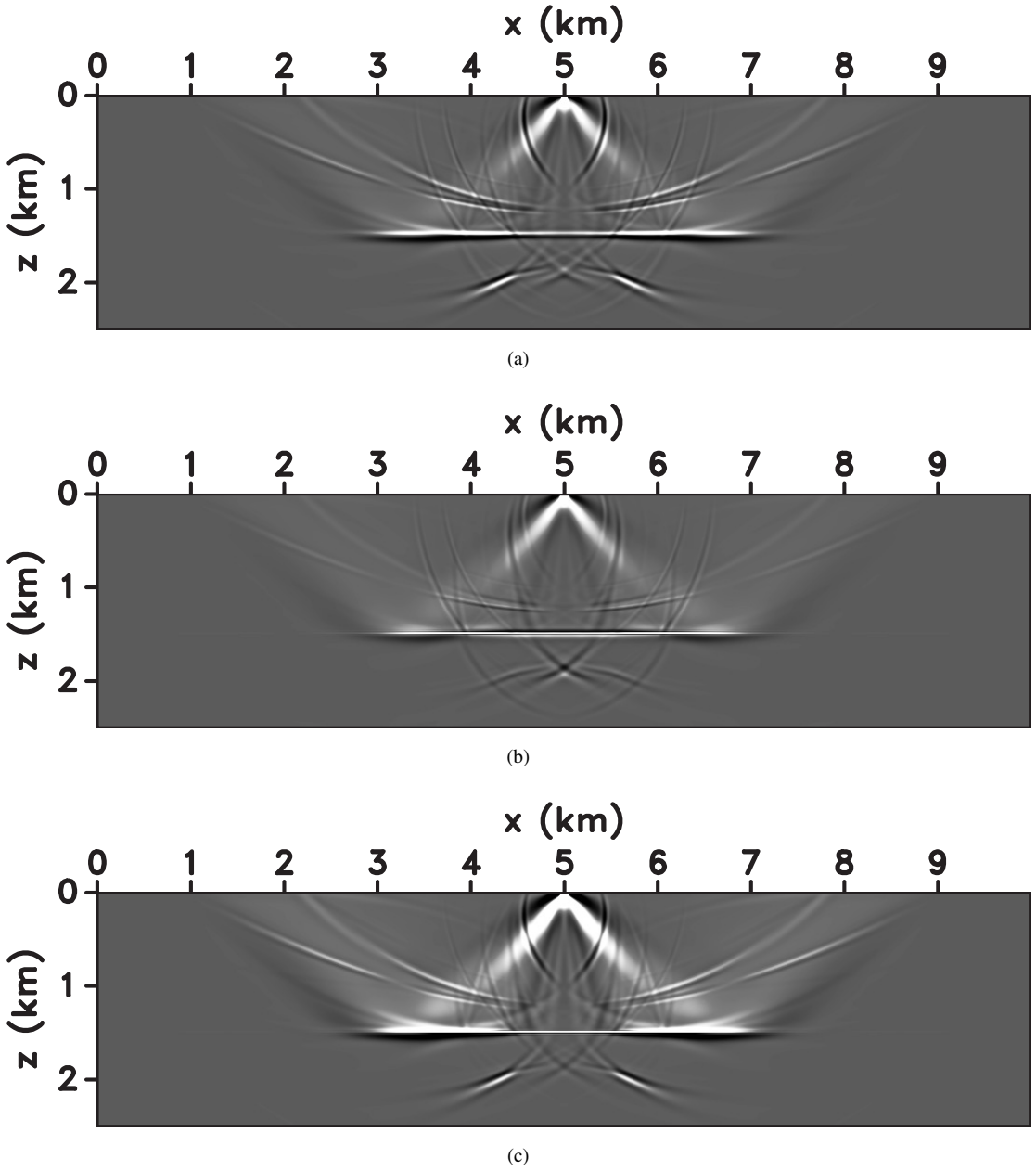


Figure 6. Individual terms of the energy imaging condition for the experiment in Figure 3 with a reflector in the migration velocity: (a) kinetic energy, (b) potential energy, and (c) total energy.

and then the Divergence Theorem A-1 to $\mathbf{F}$:

$$\int_{\Omega} \nabla\cdot\mathbf{F}d\mathbf{x} = \int_{\partial\Omega} (\mathbf{F}\cdot\mathbf{n})d\mathbf{x} = \int_{\partial\Omega} u(\nabla v\cdot\mathbf{n})d\mathbf{x} = \int_{\partial\Omega} u\frac{\partial v}{\partial\nu}d\mathbf{x}\ , \tag{A-3}$$

where $\partial v/\partial n$ is the normal derivative of v on $\partial\Omega$. This leads us to one of the Green's identities:

$$\int_{\Omega} u\nabla^2 v d\mathbf{x} + \int_{\Omega} \nabla u\cdot\nabla v d\mathbf{x} = \int_{\partial\Omega} u\frac{\partial v}{\partial\nu}d\mathbf{x}\ . \tag{A-4}$$

6.2 Conservation of energy for an acoustic wavefield

Given a solution to the acoustic wave-equation:

$$u_{tt} - c^2\nabla^2 u = 0\ , \tag{A-5}$$

where subscript t means time derivation, we can define the energy at a time t by (McOwen, 2003; Evans, 1997) as

$$E(t) = \frac{1}{2}\int_{\mathbb{R}^N} (u_t^2 + c^2|\nabla u|^2)d\mathbf{x}\ . \tag{A-6}$$

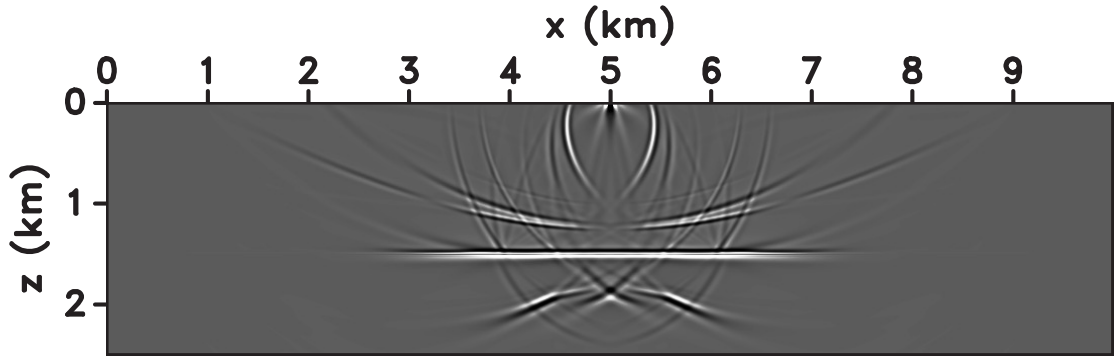


Figure 7. Same experiment of Figure 6, however, using the energy imaging condition to attenuate backscattering artifacts. Comparing with other images from Figures 4-6, except for PS and SP images (Figures 5(b) and 5(c)), this is the only image with no backscattering artifacts. This image can also be described as the subtraction between images in Figures 6(a) and 3(b).

The energy gives a integral measure of the regularity of u for first-order derivation.

Let us define the domain in which the solution is valid by $\Omega \in \mathbb{R}^N$. Considering c is a finite propagation speed, one can assume u and its derivatives are close to zero on the boundary $\partial\Omega$ for all times if Ω is sufficiently large. The conservation of energy means $\dot{E}(t) = 0$, therefore, deriving $E(t)$ within the domain Ω yields

$$\dot{E}(t) = \int_\Omega (u_t u_{tt} + c^2 \nabla u \cdot \nabla u_t) d\mathbf{x} \; . \qquad \text{(A-7)}$$

The second term in the integrand can be integrated by parts:

$$\int_\Omega c^2 (\nabla u \cdot \nabla u_t) dx = \int_\Omega c^2 \nabla \cdot (u_t \nabla u) dx - \int_\Omega c^2 (u_t \nabla^2 u) d\mathbf{x} \; . \qquad \text{(A-8)}$$

The first term of the right-hand side can be turned into a surface integral by Divergence Theorem (A-1) and then it goes to zero, since the u and its derivatives vanish on the boundary $\partial\Omega$. Substituting the remaining term in (A-7) yields

$$\dot{E}(t) = \int_\Omega u_t (u_{tt} - c^2 \nabla^2 u) d\mathbf{x} = 0 \; , \qquad \text{(A-9)}$$

because the wavefield u satisfies the wave-equation in (A-5).

6.3 Frobenius product and norm

The Frobenius norm is the most common matrix norm in numerical linear algebra. Consider an arbitrary matrix $A_{m,n}$, this norm is defined as (Golub and Loan, 1996)

$$||A||_F = \sqrt{\sum_{i=1}^{M} \sum_{j=1}^{N} |a_{ij}|^2} \; . \qquad \text{(A-10)}$$

We can also define a norm of a tensor field using the inner product of associate matrices. Given tensor fields A and B, we can define the Frobenius product:

$$< A, B >_F = A : B = \sum_{i=1}^{M} \sum_{j=1}^{N} a_{ij} b_{ij} \; , \qquad \text{(A-11)}$$

where M and N are the dimensions of the tensors A and B. This product can also be written in matrix form as

$$< A, B >_F = A : B = \text{Tr}(A^T B) = \text{Tr}(A B^T) \; . \qquad \text{(A-12)}$$

Then, we can write the Frobenius norm:

$$||A||_F = \sqrt{\text{Tr}(A A^T)} \; , \qquad \text{(A-13)}$$

6.4 Christoffel equation for isotropic media

The Christoffel equation for an anisotropic media is (Musgrave, 1970; Tsvankin, 2012)

$$\left[c_{ijkl} p_j p_l - \rho \delta_{ik} \right] u_k = 0 \; , \qquad \text{(A-14)}$$

where δ_{ij} is the Kronecker delta function, c_{ijkl} is the stiffness tensor, $\rho\,(\mathbf{x})$ is the density, u_k is the k-th component of the polarization vector $\mathbf{u}_0$, and p_j and p_l are the j-th and l-th components of the slowness vector $\mathbf{p}$. We can rewrite equation (A-14) as

$$\rho u_i = u_k c_{ijkl} p_j p_l \; . \qquad \text{(A-15)}$$

The stiffness coefficients for isotropic media are defined by

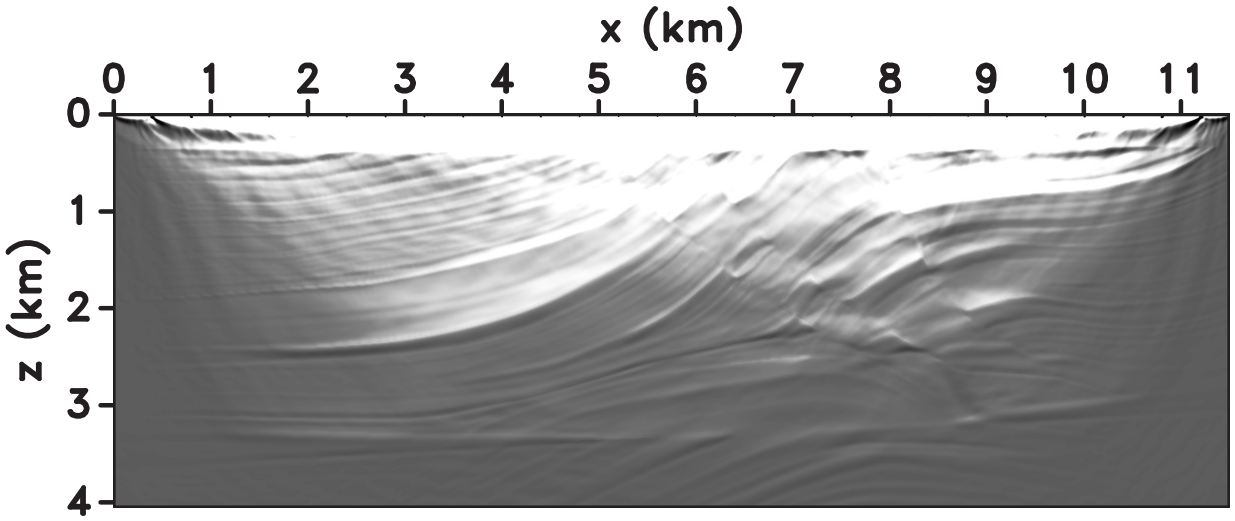
$$c_{ijlk} = \lambda \delta_{ij} \delta_{kl} + \mu \delta_{ik} \delta_{jl} + \mu \delta_{il} \delta_{jk} \; , \qquad \text{(A-16)}$$

where $\lambda\,(\mathbf{x})$ and $\mu\,(\mathbf{x})$ are the Lamé parameters. Substituting the isotropic stiffness definition in equation (A-15), we obtain

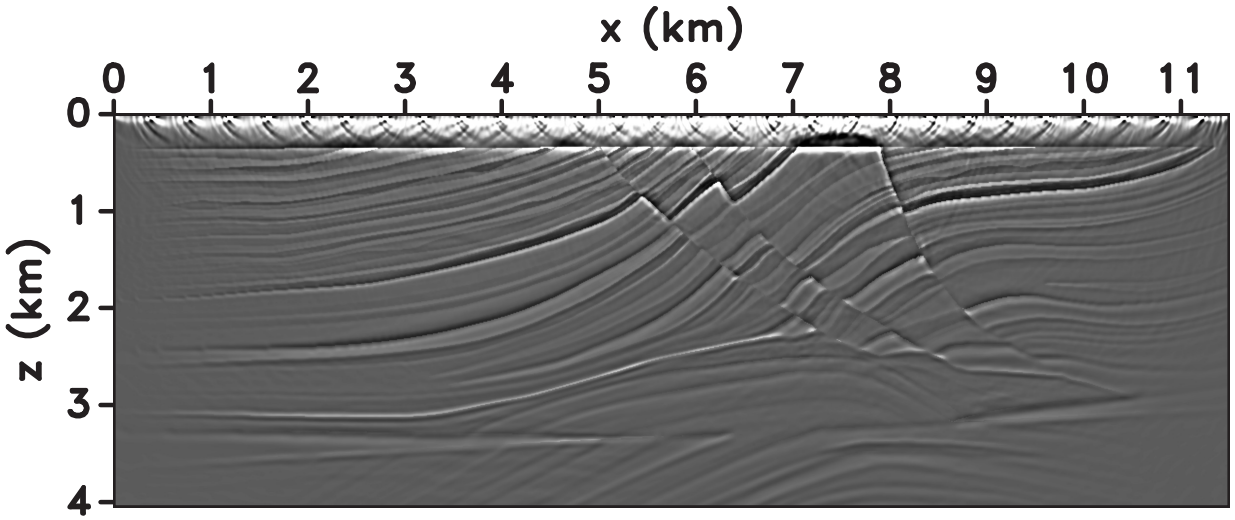
$$\begin{aligned} \rho u_i &= u_k \left(\lambda \delta_{ij} \delta_{kl} + \mu \delta_{ik} \delta_{jl} + \mu \delta_{il} \delta_{jk} \right) p_j p_l \; , & \text{(A-17)} \\ &= u_k \left(\lambda p_i p_k + \mu \delta_{ik} p_j p_j + \mu p_i p_k \right) \; , & \text{(A-18)} \\ &= \left(\lambda + \mu \right) \left(u_k p_k \right) p_i + \mu \left(p_j p_j \right) u_i \; , & \text{(A-19)} \end{aligned}$$

with summation over indices k and j. We can rewrite equation (A-19) in vector form as

$$\rho \mathbf{u}_0 = (\lambda + \mu) \left(\mathbf{u}_0 \cdot \mathbf{p} \right) \mathbf{p} + \mu (\mathbf{p} \cdot \mathbf{p}) \mathbf{u}_0 \; . \qquad \text{(A-20)}$$



(a)



(b)

Figure 8. Experiment on Marmousi model. (a) Energy imaging condition in equation (26) and (b) in equation (39). The image in (b) shows no artifacts from polarity reversal and attenuated backscattering energy compared to (a) and to conventional images.

Finally, we can also rewrite the Christoffel equation in (A-20) in terms of P and S velocities:

$$\mathbf{u}_0 = \left(v_p^2 - v_s^2\right)(\mathbf{u}_0 \cdot \mathbf{p})\,\mathbf{p} + v_s^2(\mathbf{p} \cdot \mathbf{p})\mathbf{u}_0\ . \qquad \text{(A-21)}$$